Environmental Science Processes & Impacts

ROYAL SOCIETY OF CHEMISTRY

PAPER

View Article Online
View Journal | View Issue

Check for updates

Cite this: *Environ. Sci.: Processes Impacts*, 2024, **26**, 882

Characteristics and adsorption behavior of typical microplastics in long-term accelerated weathering simulation†

Fei Yu, [a] Qiyu Qin,[a] Xiaochen Zhang[a] and Jie Ma *[bc]

Microplastics can function as carriers in the environment, absorbing various toxins and spreading to diverse ecosystems. Toxins accumulated in microplastics have the potential to be re-released, posing a threat. In this study, two typical plastics, namely polyethylene (PE) and polystyrene (PS), along with the degradable plastic poly(butylene adipate-*co*-terephthalate) (PBAT), were subjected to a long-term ultraviolet alternating weathering experiment. The study investigated the variations in the weathering process and pollutant adsorption of microplastics of different particle sizes. Furthermore, the adsorption capacity of microplastics for various pollutants was assessed. The findings indicate that particle size significantly influences weathering, leading to variations in adsorption capacity. The weathered PE displays a higher adsorption capacity for azo dyes. Additionally, the adsorption capacity of PBAT for neutral red is double that of antibiotics. Importantly, the maximum adsorption capacity of PBAT for pollutants after aging is approximately 10 times greater than that of PE. Consequently, degradable plastics undergoing weathering in the natural environment may pose a higher ecological risk than traditional plastics.

Received 7th February 2024
Accepted 13th April 2024

DOI: 10.1039/d4em00062e

rsc.li/espi

Environmental significance

Weathering experiments of microplastics (MPs) in the laboratory should simulate irradiation and temperature changes in the natural environment, and the physicochemical properties of such MPs become more similar to those in the natural environment. The ability of MPs to adsorb organic pollutants has been widely studied, and in the aquatic environment, they can act as carriers to spread pollutants over greater distances. There are differences in the accumulation effects of MPs exhibiting the same physicochemical properties on various types of organic pollutants, and the formation of composite pollution with different pollutants may have different ecological risks. In this study, PE, PS and PBAT were selected as simulated weathering objects to assess the degree of weathering of hydrocarbon plastics in the environment through CI modeling. The adsorption behavior of MPs and typical antibiotics and dyes was investigated to provide a theoretical basis for the potential ecological risk assessment of compound pollution.

Introduction

Countries around the world are trying to control the production and use of plastic to reduce ubiquitous plastic pollution. Due to improper plastic management strategies and unenforceable recycling policies,[1,2] huge amounts of plastic are discarded into the environment.[3,4] In particular, common plastics such as polyethylene (PE) and polystyrene (PS) are difficult to biodegrade[5] and their accumulation in the environment has caused harm to many ecosystems.[6–9] The degradation of plastics results in the formation of small-size plastics.Thompson *et al.*[10] referred to plastics with particle sizes less than 5 mm as microplastics (MPs).

Photooxidation, thermal aging, and mechanical damage are non-biological degradation pathways for plastics.[11,12] Among these pathways, photooxidation is considered the most significant degradation mode. When exposed to ultraviolet light, plastics undergo chemical bond breakage, leading to the introduction of oxygen atoms and the formation of carbonyl groups on the surface.[13,14] Therefore, ultraviolet irradiation is commonly employed in the laboratory to expedite the aging of microplastics, allowing for the production of microplastics that exhibit a comparable level of weathering to that found in the natural environment within a short period. This facilitates the study of the aging process of microplastics. In addition, in a water environment, reactive oxygen species ($OH\cdot$ and $O_2^{\cdot-}$) generated by light can cause the breakage of C–C bonds in the main chain of microplastics.[15] The aliphatic C–H bonds and aromatic C–H

[a]*College of Oceanography and Ecological Science, Shanghai Ocean University, No. 999, Huchenghuan Road, Shanghai, 201306, P. R. China*

[b]*School of Civil Engineering, Kashi University, Kashi 844000, China. E-mail: jma@tongji.edu.cn*

[c]*Research Center for Environmental Functional Materials, College of Environmental Science and Engineering, Tongji University, 1239 Siping Road, Shanghai, 200092, P. R. China*

† Electronic supplementary information (ESI) available: The carbonyl index calculation formula, PE-125 adsorption kinetics, DSC curve, as well as the structural formulas of PS, PE, and PBAT. See DOI: https://doi.org/10.1039/d4em00062e

bonds are partially transformed into C=O bonds, with a smaller fraction being converted to O–C=O bonds. Fenton/UV, O_3, and H_2O_2/UV processes can accelerate the aging of microplastics in a water environment;[16,17] however, it is necessary to repeatedly add oxidants to maintain a stable oxidation rate.[18] Chen *et al.* discovered that salt in seawater can facilitate the transformation of microplastic crystals and the formation of oxygen-containing functional groups. The increase in crystallinity enhances the hydrophilicity of microplastics, whereas the emergence of oxygen-containing functional groups reduces the crystallinity.[19] It is commonly believed that smaller particles possess a larger specific surface area, absorb more UV radiation energy per unit area, and are more susceptible to oxidation. In normal circumstances, the pores between particles are influenced by the particle diameter, and the greater the contact area between particles, the smaller the void created during accumulation. Due to the small particle size, only the microplastics closest to the light source can fully absorb ultraviolet radiation, potentially resulting in a lower overall aging degree for microplastics compared to those with a larger diameter.

Antibiotics such as tetracycline (TC), levofloxacin (OFL) and ciprofloxacin (CIP) are often overused in animal husbandry and aquaculture because of their broad-spectrum antimicrobial effects. Antibiotic contamination has been detected to varying degrees in streams and rivers.[22] These organic pollutants take a long time to degrade in the environment, and antibiotics can easily spread to natural water bodies,[23] leading to the development of drug resistance in bacteria.[24] The degradation products may even exhibit stronger toxicity. Another type of concern is organic dyes, which are challenging to biodegrade and exhibit high ecotoxicity. With the rapid advancement in printing and dyeing technology, synthetic chemical additives are gradually displacing natural and easily degradable substances.[25] Organic dyes have been characterized by high color intensity, elevated toxicity and low degradability. The discharge of printing and dyeing wastewater reduces dissolved oxygen in water, posing a severe and serious threat to the safety of the aquatic environment and ecosystems.[26]

Microplastics and organic pollutants coexist in water bodies, and the ability of weathered microplastics to adsorb pollutants is significantly enhanced. Hydrogen bonding, hydrophobic interactions, van der Waals forces, and electrostatic interactions are the main binding mechanisms between antibiotics and microplastics. Among them, polyamide (PA), sulfadiazine (SDZ), amoxicillin (AMX), TC, CIP, and trimethoprim (TMP) exhibit the highest adsorption capacity.[27] Zhang *et al.* discovered that weathered PS can bind to levofloxacin through π–π conjugation and hydrogen bonding.[28] The adsorption capacity of microplastics for pollutants depends, to some extent, on the characteristics of pollutants. Moura *et al.* researched the interaction between raw and aged microplastics and antibiotics across six plastic types. It was observed that hydrophobic and positively charged fluoxetine demonstrated higher adsorption on microplastics.[29] The adsorption mechanisms of various pollutants and microplastics differ. The study conducted by Wang *et al.* confirmed the bonding between dyes and PA6 through hydrogen bonding and electrostatic adsorption.[30] Liu *et al.* discovered that methylene blue and microplastic particles from single-use plastic cups were adsorbed in heterogeneous layers at low concentrations and as a monolayer with hydrophobic properties at high concentrations.[31] Mahabeer *et al.* observed that the complexation of Cl^- ions and methylene blue led to a decrease in the adsorption capacity of microplastics due to increased salinity.[32] Microplastics exhibit significant adsorption effects on antibiotics and dyes. However, it remains unclear whether various types of microplastics yield distinct adsorption effects on antibiotics and dyes. Therefore, investigating the adsorption behavior of microplastics towards different types of pollutants is essential.

PE and polystyrene PS are the most common types of plastics, frequently found in the environment where they easily adsorb environmental pollutants. PBAT, with its good biodegradability, has attracted more attention and is increasingly used in food packaging, agricultural films, and medical equipment. To investigate the variance in weathering and adsorption behaviors between non-degradable and degradable plastics, we selected PBAT as the object of our research.

In this paper, typical plastics PE, PS, and PBAT were subjected to accelerated degradation using intermittent UV radiation and cooling with ice in the dark. The weathering experiments were carried out for 60 to 120 days to provide a comprehensive insight into the degradation behavior of MPs in the environment. The study investigated the adsorption behavior of antibiotics and dyes on PE, PS, and PBAT. It also explored the differences in weathering and adsorption behavior of PE plastics with various particle sizes. The objective was to elucidate the impact of particle size on the environmental behavior of microplastics and to compare the weathering behavior of traditional plastics and degradable plastics. This research aims to provide a theoretical basis for the ecological risk assessment of microplastics at different pollution levels.

Experimental

Materials

Levofloxacin (OFL) was supplied by Shanghai Qianyan Scientific Instrument Co., Ltd (purity of 98%). Tetracycline (TC, AR) was offered by Jiangnanjie Co., Ltd. Ciprofloxacin (CIP) was supplied by Shanghai Ryon Biotechnology Co., Ltd (purity of 98%). PE (500 μm, 125 μm, and 30 μm), PS (75 μm), and PBAT (150 μm) were supplied as powders by Zhangmutou Hua Chuang Plastic Raw Materials Firm (Dongguan, China). Humic acid (HA) was obtained from Aladdin Reagent Co., Ltd (Shanghai, China). Methyl blue and neutral red were supplied by Sinopharm Chemical Reagent Co., Ltd (Shanghai, China).

The UV lamp (power of 15 W) was obtained from Hangzhou Yaguang Lighting Co., Ltd (Hangzhou, China). A thermometer (Mi Bluetooth II) was used to record temperature and humidity changes and was purchased from Taobao.

Preparation of weathered microplastics

PE (with a size of 30 μm, 125 μm, and 500 μm), PS (75 μm), and PBAT (150 μm) were weighed at 10 g and placed into Petri dishes

and labeled as PE-30, PE-125, PE-500, PS-75 and PBAT-150, respectively. All samples were placed in a radiation chamber with 4 UV lamps with 15 W irradiance. The total duration of the experiment was 120 days. The UV radiation time was 16 h, and dark treatment with cooling using ice was 8 h every day. To better explore the natural weathering process of MPs, samples were selected for FTIR analysis at 10, 20, 30, 40, 50, 60, 70, 80, 90, 100, and 120 days, respectively.

Adsorption experiments

The preliminary experiment proved that 72 h was sufficient to reach adsorption equilibrium. Adsorption experiments were conducted on pristine and aged MPs with antibiotics and dyes. The adsorption kinetic experiment was conducted at 25 °C by mixing 10 mg MPs and 20 mL pollutants with a concentration of 10 mg L^{-1} in a 50 mL conical flask. The sampling time is set at 1, 2, 4, 6, 8, 12, 24, 48 and 72 h. Meanwhile, experiments on the influence of dissolved organic matter (HA) and ionic strength (NaCl) on adsorption capacity were conducted. Adsorption isotherm experiments were conducted in the presence of HA, and OFL concentrations ranged from 5 to 40 mg L^{-1}, mixing with 5 mg L^{-1} HA. OFL maintained a concentration of 10 mg L^{-1}, and the effects of different concentrations of NaCl (0–1.0 M) on the adsorption were determined. Besides, the pH of the solution was adjusted to 6–7 using 0.1 M NaOH and 0.1 M HCl.

All the experiments were carried out in a constant temperature shaker (TS-350C, China) at 150 rpm. After adsorption experiments, all the solutions were filtered through a 0.22 μm aqueous membrane filter. The TC, OFL, CIP, methyl blue and neutral red concentrations in solution were analyzed using a UV-visible spectrophotometer (UV-2900, Hitachi, Japan) at a wavelength of 275.4 nm, 287.6 nm, 294 nm, 664 nm and 553 nm, respectively. All the above experiments were set to be repeated three times, and the mean values of the experimental data were considered the ultimate results. The adsorption kinetics of PE-125 for OFL is shown in Fig. S1.†

Characterization

The surface morphology of pristine and aged MPs was analyzed by scanning electron microscopy (SEM, Zeiss Sigma 300, UK) at 3.0 kV. Attenuated total reflectance Fourier transform infrared spectroscopy (ATR-FTIR) identified the surface chemical characteristics with a wavenumber of 4000–600 cm^{-1} (Thermo Fisher, Nicolet Is10). Besides, a thermogravimetric analyzer (Simultaneous DSC-TGA Q600, America) was used to analyze the thermal stability changes of the samples, performed under a N_2 atmosphere at a rate of 10 °C min^{-1} from 50 to 600 °C.

Results and discussion

Morphology of MPs

The morphologies of the pristine and UV-treated PE, PS, and PBAT samples are depicted in Fig. 1. The pristine PE and PS particles are approximately spherical and massive, respectively, with smooth surfaces. The appearance of cracks caused

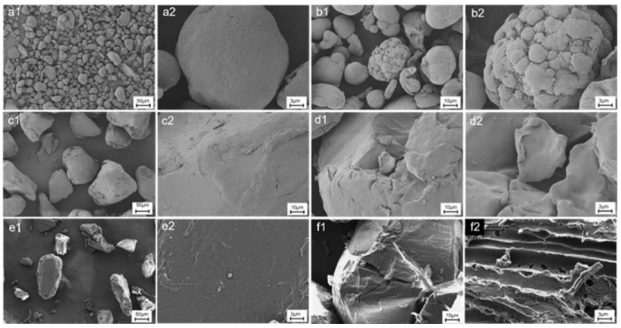

Fig. 1 SEM images of microplastics before and after UV weathering, (a1 and a2) pristine PE; (b1 and b2) PE weathered for 120 days; (c1 and c2) pristine PS; (d1 and d2) PS weathered for 60 days; (e1 and e2) pristine PBAT; (f1 and f2) PBAT weathered for 120 days.

morphology variations during UV treatment. As the UV exposure time increased, the surface roughness of MPs increased. After 120 days of UV treatment, PE presented a distinct weathering phenomenon, with spherical cracks appearing on its surface. At the same time, smaller debris occurred following weathering. The findings revealed that UV exposure time is a vital factor in plastic degradation. The textures of PS samples became rough and generated flakes after 60 days. Delamination following weathering was linked to the formation of a brittle surface area and particle surface layer,[20] consistent with the conclusion that cracks and flakes are common degradation modes. After 120 days of UV exposure, a stratified structure as well as a large number of wrinkles and holes appeared on the surface of PBAT, effectively increasing the attachment points for pollutants. It may be because PBAT contains oxygen-containing functional groups, leading to more intense weathering under the same conditions. The degradation mechanism requires further studies, but it can be confirmed that the changes in surface morphology can provide more adsorption sites for pollutants.[21,33,34] The degradation of a polymer is related to its properties. The plastic structures are presented in Table S1.† PE and PS have backbones that are completely built of carbon atoms making them resistant to the cleavage of chemical bonds.[35] In contrast, the main chain of PBAT is made of oxygen atoms, making it more prone to degradation through the hydrolytic cleavage of chemical bonds.

Chemical composition

The three types of MPs underwent photooxidation reactions to different degrees after UV irradiation. The higher the light utilization and oxygen content, the greater the weathering degree. The changes in oxygen-containing functional groups of PE with different diameters are presented in Fig. 2a and b. Two adsorption peaks at 2920 cm^{-1} and 2850 cm^{-1} are associated with the asymmetric and symmetric stretching vibrations of $-CH_2$, respectively.[16] The adsorption peaks at 1470 cm^{-1} and 720 cm^{-1} represent bending stretching vibrations of $-CH_2$. It can be observed that regardless of the duration of PE, the three characteristic peak bands did not change significantly. But a new characteristic peak of the C=O bond was observed at

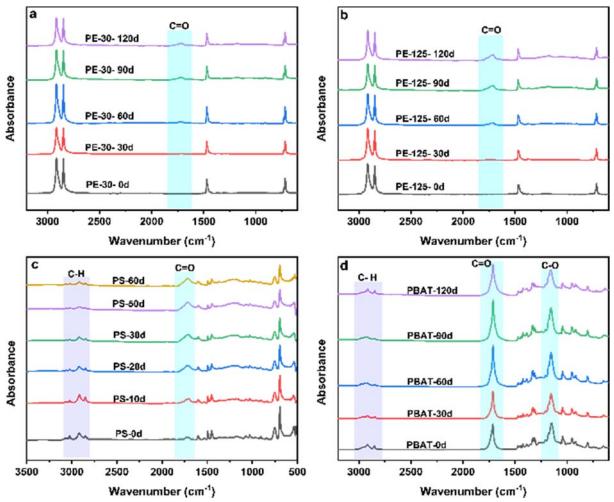

Fig. 2 The FTIR images of MPs, (a) PE-30; (b) PE-125; (c) PS-75; (d) PBAT-150.

1720 cm^{-1}. As the exposure time increased, the area of the characteristic peak also visibly increased. By integrating the peak area of C=O, the carbonyl index (CI) value was found to be stable in 110–120 days, indicating that the photooxidation reaction was in equilibrium. Meanwhile, the CI values of PE-30 and PE-125 reached 0.85 and 2.2, respectively. PE is composed of ethylene and does not contain oxygen-containing functional groups. The generation of oxygen-containing functional groups and the enhancement of vibration intensity mean an increasing degree of weathering. The CI value and exposure time have good regularity, so a linear model of CI change with weathering time can be established.

The FTIR spectra of the weathering process of PS are presented in Fig. 2c. A new peak appeared near 1720 cm^{-1}, and the intensity of peaks in the range of 3100 cm^{-1}-2800 cm^{-1} gradually decreased. However, there is no significant difference in the spectrum at 1500–1400 cm^{-1}, which are identified as the carbonyl vibration peak,[36] the C–H stretching vibration peak on the benzene ring, and the C–H bending vibration peak. These results indicate that the C–H bond of PS changed to varying degrees during the photooxidation.[37] Under UV processing, the color of PS changes from white to dark yellow, indicating a change in the chemical composition of the surface layer. Photoinduced oxidation of PS occurs more readily in the air than in water, confirming that UV exposure plays a dominant role in the generation of oxygen-containing functional groups.[38] Fig. 3d shows FTIR spectra of different oxidation degrees of PBAT. The peaks at 3000–2800 cm^{-1}, 1780–1667 cm^{-1} and 1200–1090 cm^{-1} are identified as the characteristic bands of the PBAT structure, including C–H vibrations on the benzene ring, C=O and O–C–O vibrations. The vibration intensity of C–H decreased as the weathering time increased, indicating that the carbon chains have been cross-linked or rearranged. The variation in the trend of oxygen-containing functional groups of PBAT with the weathering degree is shown in Fig. S2.† In the initial stage, the oxygen content of C–O and C=O increased rapidly. The content of C=O eventually stabilized, while the relative proportion of C–H decreased. The free radicals created from the cleavage of C–C bonds (375 kJ mol^{-1}) and C–H bonds (420 kJ mol^{-1}) by UV irradiation were able to generate C=C bonds, C=O bonds or –OH groups, leading to chain scission and crosslinking, chain propagation, chain branching and chain termination.[20]

Thermal stability and crystallinity

Thermogravimetric analysis is of great significance in studying the thermal stability of microplastics. Fig. 3a illustrates the weight loss processes of PE-125 particles before and after weathering. The pyrolysis of PE at different exposure times all showed two weight loss processes. The weight loss ratio of the first stages is 10.2%, 18.4%, and 22.4% at 200–457 °C, 195–446 °C, and 100–427 °C, respectively, indicating that the thermal stability of PE decreases obviously after weathering due to the production of low boiling point small molecules. The longer the weathering time, the higher the weight loss rate. Another view is that the increased moisture content of the particles results in more weight loss. After weathering, smaller particle sizes and a rougher surface morphology can access more water vapor in the air. The weight loss ratio of the second part is 89.8%, 84.6%, and 74.6% at 457–493 °C, 446–495 °C, and 427–498 °C, respectively. The samples were completely pyrolyzed near 500 °C, but a small amount of ash remained in those exposed for 120 days, which could be impurities mixed in during the prolonged

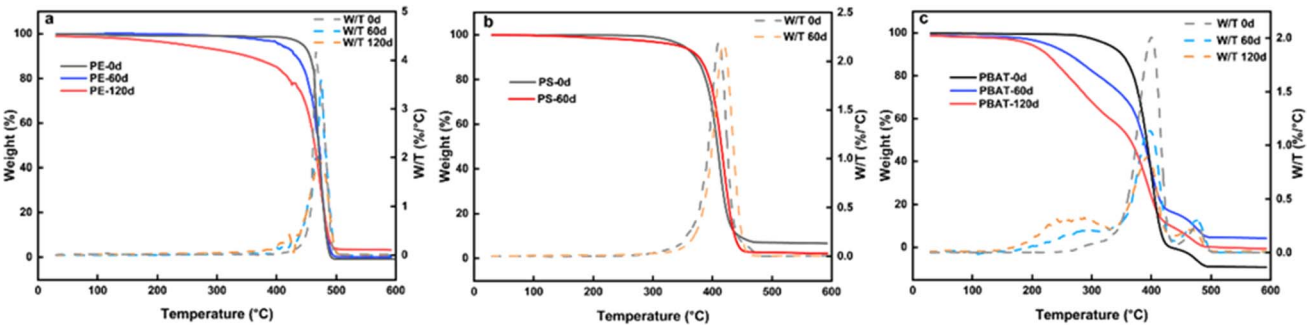

Fig. 3 TGA-DTG diagrams of three microplastics, (a) TGA-DTG of PE with different weathering times; (b) TGA-DTG of microplastic PS; (c) TGA-DTG of degradable microplastic PBAT.

exposure. Crystallinity is often used to reflect the range of polymer crystalline regions. Based on the DSC curve data, the crystallinity of virginal PE samples is 13.0%, while the crystallinity of PE after accelerated weathering for 120 days is 47.1% as determined by integration (Fig. S3a†). During the accelerated weathering process, the unstable non-crystalline regions are destroyed, leaving behind the more stable crystalline regions. As a result, the weathered PE was more stable and affected the adsorption performance of pollutants. These findings indicate that weathered microplastics pose a greater ecological risk.

As shown in Fig. 3b, the PS samples remain relatively stable before and 60 days of weathering. However, the DTG curve shows that the peak of weathered PS has shifted to a higher temperature, which means that thermal stability is enhanced. PS particles are stratified and the surface fragments fall off, resulting in a decrease in the content of the amorphous structure. Fig. S3b† shows that the endothermic peak temperature of the original PS was 416 °C, while the melting peak temperature (T_m) increased to 424 °C after 60 days of weathering, slightly deviating from a typical endothermic peak range of 440–450 °C.[39] It was found that T_m progressively increased gradually with prolonged weathering, resulting in enhanced thermal stability. Given that PS is a highly crystalline polymer, the variations in T_m could be ascribed to changes in crystallinity.[40] Because of the surface peeling phenomenon, the carbon chains remaining necessitate more energy for decomposition upon melting.[41] To sum up, the residual microplastics following UV weathering are resistant to degradation and are more prone to generating persistent composite pollution effects from microplastic pollutants.

Degradable microplastic PBAT is an amorphous polymer.[42] The PBAT particles exhibit weight loss decomposition at 200–400 °C both before and after weathering. The peak of PBAT after weathering migrated to lower temperature. This result suggested that PBAT may degrade under abiotic factors. Under UV treatment, the carbon chains of PBAT are cross-linked and the structure containing benzophenone is induced.[43] These processes can promote subsequent biodegradation. Therefore, the thermal stability decreases during the weathering process.

Weathering process and model

The CI prediction model for PE is shown in Fig. 4. The percentage of oxygen in the polymer is used to reflect the level of plastic degradation, and the CI value serves as an important indicator to describe the C/O ratio.[44] CI values of two different sizes of microplastics visibly increased with increasing weathering time and showed a strong linear fit. The R^2 value for the CI model with a particle size of 30 μm is 0.978, while that for PE-125 is 0.99. Assessing the weathering time of microplastics in the environment can help evaluate their toxic effects. The model can predict the residence time of MPs in the environment, significantly improving the accuracy of risk assessment. By comparing the CI linear fitting slopes of the two particle sizes of PE, it is observed that the slope of PE-125 is larger, indicating a faster photooxidation rate. Our hypothesis is that the finer particles may shield each other, reducing the unit area exposed to UV radiation. To validate the precision and feasibility of the model, CI values of PE at 80 days, 90 days, and 100 days were predicted according to the linear model (Table S2†). The predicted CI values of PE in 80 days, 90 days, and 100 days were in line with the measured values ($\sigma < 0.09$).

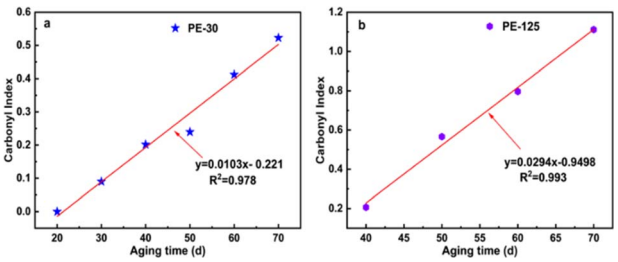

Fig. 4 Model of CI for microplastic PE with different particle sizes during the weathering process, (a) PE-30; (b) PE-125.

Adsorption behavior of microplastics and various pollutants

The adsorption behavior of PE with different particle sizes for various types of pollutants is shown in Fig. 5. PE with a particle size of 125 μm showed the highest adsorption capacity for all pollutants. Both pristine and weathered PE-125 exhibited the highest adsorption capacity for OFL, methylene blue, and neutral red. It is generally believed that the smaller the size of microplastics, the larger the specific surface area, and more adsorption sites can be provided. However, this study showed the opposite result, possibly due to the agglomeration of PE-30 powder particles.[45] It can also be noticed that the adsorption capacity of weathered PE is improved compared to its original state. This improvement can be attributed to the increased presence of oxygen-containing functional groups in PE after weathering, enhancing the hydrophilicity of PE. The adsorption of TC and OFL by PE mainly relies on hydrogen bonding. Compared with water-soluble antibiotics, the weathered PE has a higher adsorption capacity for dyes, which is because more

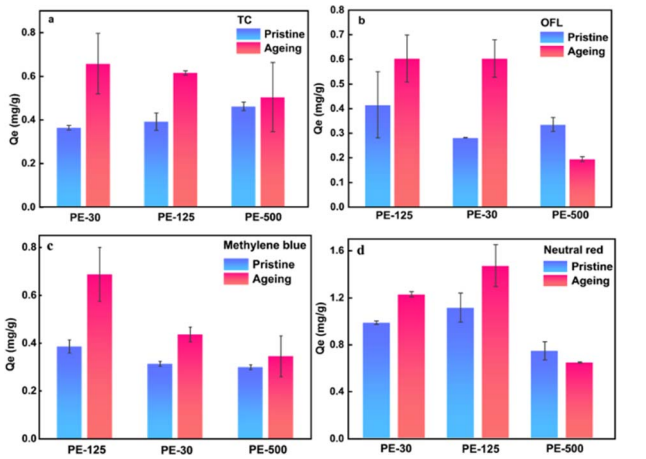

Fig. 5 Adsorption behavior before and after weathering PE with antibiotics and dyes with different particle sizes, (a) TC adsorption on PE; (b) OFL adsorption on PE; (c) methylene blue adsorption on PE; (d) neutral red adsorption on PE.

cracks and pores appear on the aged PE. Methylene blue and neutral red can permeate the interior of MPs and bind through physical adsorption.

TC is considered an amphoteric molecule with numerous ionizable functional groups, and its adsorption capacity reaches its maximum when pH = 6.[46] TC primarily exists in cationic form as the pH decreases and shifts to anionic form with increasing pH. The zeta potential of PE before and after weathering at pH = 3 was 0.63 and −1.24, respectively. At pH = 9, the zeta potentials were −28.1 and −30.4, respectively. Thus, TC will produce electrostatic repulsion on the surface of PE particles, and OFL also shows a similar trend. OFL is positively charged by protonation in the acidic range, while under the alkaline conditions, it shows electrostatic action to inhibit the adsorption behavior. Therefore, PE displayed limited adsorption capacity for antibiotics in this study.

The adsorption performance of PS with antibiotics and dyes is displayed in Fig. 6(a and b). The adsorption capacity of PS for dyes is higher than that for antibiotics. The original PS adsorbs pollutants mainly through hydrophobic and π–π co-electron interaction. The photooxidation reaction accelerates weathering processes, resulting in introduction of C=O, C–O, or O–H groups that alter the physicochemical properties of MPs, thereby enhancing hydrogen bonding between MPs and pollutants. Hence, the adsorption capacity of PS for pollutants is significantly enhanced by UV radiation. After aging, the equilibrium adsorption capacity of PS for TC, CIP, neutral red, and methylene blue increased by 58% (0.69–1.09 mg g^{-1}), 138% (1.72–4.09 mg g^{-1}), 381% (0.85–4.09 mg g^{-1}) and 469% (0.97–5.52 mg g^{-1}), respectively. The adsorption capacity of PBAT was significantly different before and after weathering (Fig. 6c and d). After long-term accelerated weathering, PBAT showed substantial pollutant enrichment. The equilibrium adsorption capacity of PBAT for CIP was increased from 0.62 mg g^{-1} to 6.22 mg g^{-1} and for neutral red it increased from 2.92 mg g^{-1} to 12.70 mg g^{-1}.

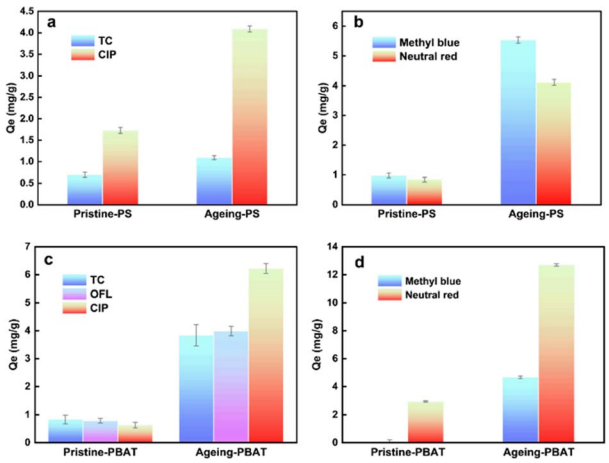

Fig. 6 Adsorption behavior before and after weathering PS and PBAT with pollutants. (a) Antibiotic (TC and CIP) adsorption on PS; (b) dye (methyl blue and neutral red) adsorption on PS; (c) antibiotic (TC, OFL, and CIP) adsorption on PBAT; (d) dye (methyl blue and neutral red) adsorption on PBAT.

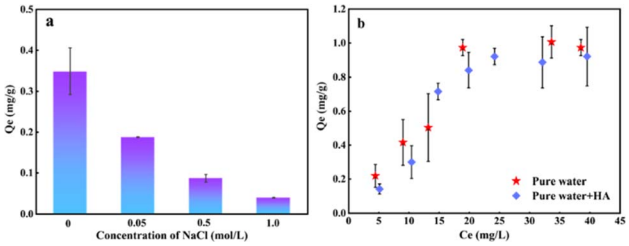

Fig. 7 Effects of different environmental factors on the adsorption of OFL by PE-125 (a) NaCl; (b) HA.

In general, the above results show that weathered MPs exhibit a stronger adsorption capacity for dyes compared to antibiotics. Under the same weathering conditions, PBAT shows a high adsorption capacity for pollutants, which may be because the appearance of folds, wrinkles, and pores on the surface of PBAT provides more adsorption sites (Fig. 1f). This suggests that PBAT has a stronger pollutant loading capacity than conventional microplastics. This result is consistent with that by Zuo *et al.*[42] While promoting biodegradable plastics, it is also necessary to try to avoid the harm caused by their degradation in the natural environment.

The CI index indicates that the oxidation degree of PE-125 was more intense at the same treatment time, leading to a higher presence of oxygen-containing functional groups on the surface that facilitated the interaction with organic pollutants. Therefore, choosing PE-125 with a high degree of weathering can better demonstrate the differences in adsorption under the influence of environmental factors. As can be seen from Fig. 7 the maximum adsorption capacity of the weathered PE-125 samples to hydrophilic organic matter OFL is 0.35 mg g^{-1} in pure water. With an increase in the sodium chloride concentration the adsorption behavior was inhibited. The ionic competition between salt ions and pollutants weakens the adsorption capacity of microplastics.[47] Zeta potential analysis confirmed that surface electronegativity of weathered MPs is attributed to charge accumulation. This is following Liu's research.[48] It is observed from Fig. 7b that the presence of organic matter will also reduce the adsorption capacity of microplastics to antibiotics. Humic acid (HA) contains many aromatic substances, and the active functional groups on HA have hydrophobic interaction[49] and complexation[50] with microplastics. Therefore, the interfacial interaction between microplastics and OFL is weakened. In addition, HA can interact with hydrophilic and polar organic compounds through complexation and hydrogen bonding.

Conclusions

This article simulated the accelerated weathering process of PE, PS, and PBAT under environmental conditions and focused on the changes in surface morphology, chemical composition, and material properties. The CI prediction model for PE presented a strong linear relationship with the weathering time ($R^2 > 0.97$) and could predict the subsequent change in the CI value

relatively accurately. The adsorption behavior of PE showed that the surface morphology changes and increased hydrogen bonding enhanced the adsorption capacity of weathered microplastics. Additionally, the ion concentration and dissolved organic matter (DOM) competed with microplastics for adsorption, resulting in lower adsorption performance of weathered microplastics in complex natural environments compared to pure water environments. Interestingly, all three plastics showed extremely high adsorption capacity for dyes after weathering. Due to the presence of heteroatoms in PBAT, chemical weathering is more likely to occur, and the weathered PBAT could be a good carrier of organic pollutants in fresh water. We recommend monitoring the presence of microplastics in dye wastewater to prevent their release into nature as composite pollutants. Further research on the environmental behavior of PBAT in other ecosystems is necessary to comprehensively understand the weathering of degradable plastics in the environment and associated ecological risks.

Author contributions

Fei Yu: investigation, resources, writing – original draft, Qiyu Qin: investigation, writing – original draft, Xiaochen Zhang: formal analysis, methodology, and Jie Ma: conceptualization, writing – review & editing, supervision.

Conflicts of interest

There are no conflicts to declare.

Acknowledgements

This research was supported by the National Natural Science Foundation of China (22276137, 52170087) and the Fundamental Research Funds for the Central Universities (XJEDU2023Z009). We are also thankful to the anonymous reviewers for their valuable comments on improving this manuscript.

Notes and references

1 S. B. Borrelle, J. Ringma, K. L. Law, C. C. Monnahan, L. Lebreton, A. McGivern, E. Murphy, J. Jambeck, G. H. Leonard, M. A. Hilleary, M. Eriksen, H. P. Possingham, H. De Frond, L. R. Gerber, B. Polidoro, A. Tahir, M. Bernard, N. Mallos, M. Barnes and C. M. Rochman, Predicted growth in plastic waste exceeds efforts to mitigate plastic pollution, *Science*, 2020, **369**, 1515.

2 M. MacLeo, H. P. H. Arp, M. B. Tekman and A. Jahnke, The global threat from plastic pollution, *Science*, 2021, **373**, 61–65.

3 M. Bergmann, S. Mutzel, S. Primpke, M. B. Tekman, J. Trachsel and G. Gerdts, White and wonderful? Microplastics prevail in snow from the Alps to the Arctic, *Sci. Adv.*, 2019, **5**, eaax1157.

4 D. Zhu, J. Ma, G. Li, M. C. Rillig and Y. G. Zhu, Soil plastispheres as hotpots of antibiotic resistance genes and potential pathogens, *Multidisciplinary J. Microb. Ecol.*, 2021, **16**, 521–532.

5 A. Stubbins, K. L. Law, S. E. Munoz, T. S. Bianchi and L. X. Zhu, Plastics in the Earth system, *Science*, 2021, **373**, 51–55.

6 F. Gallo, C. Fossi, R. Weber, D. Santillo, J. Sousa, I. Ingram, A. Nadal and D. Romano, Marine litter plastics and microplastics and their toxic chemicals components: the need for urgent preventive measures, *Environ. Sci. Eur.*, 2018, **30**, 13.

7 A. J. R. Watts, C. Lewis, R. M. Goodhead, S. J. Beckett, J. Moger, C. R. Tyler and T. S. Galloway, Uptake and Retention of Microplastics by the Shore Crab Carcinus maenas, *Environ. Sci. Technol.*, 2014, **48**, 8823–8830.

8 Y. M. Luo, L. Z. Li, Y. D. Feng, R. J. Li, J. Yang, W. Peijnenburg and C. Tu, Quantitative tracing of uptake and transport of submicrometre plastics in crop plants using lanthanide chelates as a dual-functional tracer, *Nat. Nanotechnol.*, 2022, **17**, 424.

9 G. Malafaia, I. F. Nascimento, F. N. Estrela, A. T. B. Guimaraes, F. Ribeiro, T. M. da Luz and A. S. D. Rodrigues, Green toxicology approach involving polylactic acid biomicroplastics and neotropical tadpoles: (Eco)toxicological safety or environmental hazard?, *Sci. Total Environ.*, 2021, **783**, 146994.

10 R. C. Thompson, Y. Olsen, R. P. Mitchell, A. Davis, S. J. Rowland, A. W. John, D. McGonigle and A. E. Russell, Lost at sea: where is all the plastic?, *Science*, 2004, **304**, 838.

11 O. S. Alimi, D. Claveau-Mallet, R. S. Kurusu, M. Lapointe, S. Bayen and N. Tufenkji, Weathering pathways and protocols for environmentally relevant microplastics and nanoplastics: What are we missing?, *J. Hazard. Mater.*, 2022, **423**, 126955.

12 J. Ge, M. Wang, P. Liu, Z. Zhang, J. Peng and X. Guo, A systematic review on the aging of microplastics and the effects of typical factors in various environmental media, *TrAC, Trends Anal. Chem.*, 2023, **162**, 117025.

13 L. Q. Cai, J. D. Wang, J. P. Peng, Z. Q. Wu and X. L. Tan, Observation of the degradation of three types of plastic pellets exposed to UV irradiation in three different environments, *Sci. Total Environ.*, 2018, **628–629**, 740–747.

14 Y. K. Song, S. H. Hong, S. Eo and W. J. Shim, The fragmentation of nano- and microplastic particles from thermoplastics accelerated by simulated-sunlight-mediated photooxidation, *Environ. Pollut.*, 2022, **311**, 119847.

15 J. Hu, F. Y. Lim and J. Hu, Characteristics and behaviors of microplastics undergoing photoaging and Advanced Oxidation Processes (AOPs) initiated aging, *Water Res.*, 2023, **232**, 119628.

16 M. Lang, X. Yu, J. Liu, T. Xia, T. Wang, H. Jia and X. Guo, Fenton aging significantly affects the heavy metal adsorption capacity of polystyrene microplastics, *Sci. Total Environ.*, 2020, **722**, 137762.

17 J. Meng, B. L. Xu, F. Liu, W. J. Li, N. Sy, X. X. Zhou and B. Yan, Effects of chemical and natural ageing on the release of potentially toxic metal additives in commercial PVC microplastics, *Chemosphere*, 2021, **283**, 131274.

18 P. Liu, Y. Shi, X. Wu, H. Wang, H. Huang, X. Guo and S. Gao, Review of the artificially-accelerated aging technology and ecological risk of microplastics, *Sci. Total Environ.*, 2021, **768**, 144969.
19 Q. Chen, Q. Wang, C. Zhang, J. Zhang, Z. Dong and Q. Xu, Aging simulation of thin-film plastics in different environments to examine the formation of microplastic, *Water Res.*, 2021, **202**, 117462.
20 L. Cai, J. Wang, J. Peng, Z. Wu and X. Tan, Observation of the degradation of three types of plastic pellets exposed to UV irradiation in three different environments, *Sci. Total Environ.*, 2018, **628–629**, 740–747.
21 B. Abaroa-Perez, S. Ortiz-Montosa, J. J. Hernandez-Brito and D. Vega-Moreno, Yellowing, Weathering and Degradation of Marine Pellets and Their Influence on the Adsorption of Chemical Pollutants, *Polymers*, 2022, **14**, 1305.
22 M. C. Danner, A. Robertson, V. Behrends and J. Reiss, Antibiotic pollution in surface fresh waters: Occurrence and effects, *Sci. Total Environ.*, 2019, **664**, 793–804.
23 L. Xu, H. Zhang, P. Xiong, Q. Zhu, C. Liao and G. Jiang, Occurrence, fate, and risk assessment of typical tetracycline antibiotics in the aquatic environment: A review, *Sci. Total Environ.*, 2021, **753**, 141975.
24 J. Jia, Y. Guan, M. Cheng, H. Chen, J. He, S. Wang and Z. Wang, Occurrence and distribution of antibiotics and antibiotic resistance genes in Ba River, China, *Sci. Total Environ.*, 2018, **642**, 1136–1144.
25 Y. Tu, G. Shao, W. Zhang, J. Chen, Y. Qu, F. Zhang, S. Tian, Z. Zhou and Z. Ren, The degradation of printing and dyeing wastewater by manganese-based catalysts, *Sci. Total Environ.*, 2022, **828**, 154390.
26 Q. Liu, Y. Li, H. Chen, J. Lu, G. Yu, M. Möslang and Y. Zhou, Superior adsorption capacity of functionalised straw adsorbent for dyes and heavy-metal ions, *J. Hazard. Mater.*, 2020, **382**, 121040.
27 J. Li, K. Zhang and H. Zhang, Adsorption of antibiotics on microplastics, *Environ. Pollut.*, 2018, **237**, 460–467.
28 Y. Zhang, Y. Li, Y. Wang, F. Su, J. Qian and S. Liu, Adsorption of levofloxacin by ultraviolet aging microplastics, *Chemosphere*, 2023, **343**, 140196.
29 D. S. Moura, C. J. Pestana, C. F. Moffat, N. Gkoulemani, J. Hui, J. T. S. Irvine and L. A. Lawton, Aging microplastics enhances the adsorption of pharmaceuticals in freshwater, *Sci. Total Environ.*, 2024, **912**, 169467.
30 K. Wang, Y. Kou, K. Wang, S. Liang, C. Guo, W. Wang, Y. Lu and J. Wang, Comparing the adsorption of methyl orange and malachite green on similar yet distinct polyamide microplastics: Uncovering hydrogen bond interactions, *Chemosphere*, 2023, **340**, 139806.
31 L. Liu, H. Ma and B. Xing, Aging and characterization of disposable polypropylene plastic cups based microplastics and its adsorption for methylene blue, *Chemosphere*, 2024, **349**, 140976.
32 J. Mahabeer, U. Kumari, D. Lokhat, M. Carsky and B. C. Meikap, Implementation of microplastics derived from waste plastic for uptake of MB dye: Performance and LCA study, *Desalination*, 2023, **546**, 116214.
33 X. Fan, Y. Zou, N. Geng, J. Liu, J. Hou, D. Li, C. Yang and Y. Li, Investigation on the adsorption and desorption behaviors of antibiotics by degradable MPs with or without UV ageing process, *J. Hazard. Mater.*, 2021, **401**, 123363.
34 X. Fan, R. Gan, J. Liu, Y. Xie, D. Xu, Y. Xiang, J. Su, Z. Teng and J. Hou, Adsorption and desorption behaviors of antibiotics by tire wear particles and polyethylene microplastics with or without aging processes, *Sci. Total Environ.*, 2021, **771**, 145451.
35 Y. Zheng, E. K. Yanful and A. S. Bassi, A review of plastic waste biodegradation, *Crit. Rev. Biotechnol.*, 2005, **25**, 243–250.
36 X. X. Han, R. D. Vogt, J. Y. Zhou, B. Y. Zheng, X. Yu, J. F. Feng and X. Q. Lu, Increased Cu(II) Adsorption Onto UV-Aged Polyethylene, Polypropylene, and Polyethylene Terephthalate Microplastic Particles in Seawater, *Front. Mar. Sci.*, 2021, **8**, 770606.
37 L. Ding, R. F. Mao, S. R. Ma, X. T. Guo and L. Y. Zhu, High temperature depended on the ageing mechanism of microplastics under different environmental conditions and its effect on the distribution of organic pollutants, *Water Res.*, 2020, **174**, 115634.
38 J. Wu, P. Xu, Q. Chen, D. Ma, W. Ge, T. Jiang and C. Chai, Effects of polymer aging on sorption of 2,2',4,4'-tetrabromodiphenyl ether by polystyrene microplastics, *Chemosphere*, 2020, **253**, 126706.
39 A. H. Farha, A. F. Al Naim and S. A. Mansour, Thermal Degradation of Polystyrene (PS) Nanocomposites Loaded with Sol Gel-Synthesized ZnO Nanorods, *Polymers*, 2020, **12**, 1935.
40 L. Zhou, T. Wang, G. Qu, H. Jia and L. Zhu, Probing the aging processes and mechanisms of microplastic under simulated multiple actions generated by discharge plasma, *J. Hazard. Mater.*, 2020, **398**, 122956.
41 O. A. Serenko, V. I. Roldughin, A. A. Askadskii, E. S. Serkova, P. V. Strashnov and Z. B. Shifrina, The effect of size and concentration of nanoparticles on the glass transition temperature of polymer nanocomposites, *RSC Adv.*, 2017, **7**, 50113–50120.
42 L. Z. Zuo, H. X. Li, L. Lin, Y. X. Sun, Z. H. Diao, S. Liu, Z. Y. Zhang and X. R. Xu, Sorption and desorption of phenanthrene on biodegradable poly(butylene adipate co-terephtalate) microplastics, *Chemosphere*, 2019, **215**, 25–32.
43 G. X. De Ho, M. T. Zumstein, G. J. Getzinger, I. Ruegsegger, H. P. E. Kohler, M. A. Maurer-Jones, M. Sander, M. A. Hillmyer and K. McNeill, Photochemical Transformation of Poly(butylene adipate-co-terephthalate) and Its Effects on Enzymatic Hydrolyzability, *Environ. Sci. Technol.*, 2019, **53**, 2472–2481.
44 J. Brandon, M. Goldstein and M. D. Ohman, Long-term aging and degradation of microplastic particles: Comparing *in situ* oceanic and experimental weathering patterns, *Mar. Pollut. Bull.*, 2016, **110**, 299–308.
45 A. Turner and L. A. Holmes, Adsorption of trace metals by microplastic pellets in fresh water, *Environ. Chem.*, 2015, **12**, 600–610.

46 B. L. Xu, F. Liu, P. C. Brookes and J. M. Xu, Microplastics play a minor role in tetracycline sorption in the presence of dissolved organic matter, *Environ. Pollut.*, 2018, **240**, 87–94.
47 J. Li, K. Zhang and H. Zhang, Adsorption of antibiotics on microplastics, *Environ. Pollut.*, 2018, **237**, 460–467.
48 P. Liu, K. Lu, J. Li, X. Wu, L. Qian, M. Wang and S. Gao, Effect of aging on adsorption behavior of polystyrene microplastics for pharmaceuticals: Adsorption mechanism and role of aging intermediates, *J. Hazard. Mater.*, 2020, **384**, 121193.
49 A. Abdurahman, K. Y. Cui, J. Wu, S. C. Li, R. Gao, J. Dai, W. Q. Liang and F. Zeng, Adsorption of dissolved organic matter (DOM) on polystyrene microplastics in aquatic environments: Kinetic, isotherm and site energy distribution analysis, *Ecotoxicol. Environ. Saf.*, 2020, **198**, 110658.
50 M. Zhang, J. H. Yang, Z. Kang, X. Y. Wu, L. F. Tang, Z. M. Qiang, D. Y. Zhang and X. L. Pan, Removal of micron-scale microplastic particles from different waters with efficient tool of surface-functionalized microbubbles, *J. Hazard. Mater.*, 2021, **404**, 124095.

